An Alternative Mechanistic Paradigm for the β-(Z)-Hydrosilylation of Terminal Alkynes: The Role of Acetone as Silane Shuttle

Manuel Iglesias,*a Pablo J. Sanz Miguel,a Victor Polo,b Francisco J. Fernández-Alvarez,*a Jesús J. Pérez-Torrente,a and Luis A. Oro*a

Abstract: The β-(Z)-selectivity in hydrosilylation of terminal alkynes has been hitherto explained by introduction of isomerisation steps in classical mechanisms. DFT calculations and experimental observations on the system [M(I)2{κ-C,C,O,O-bis(NHC)}]BF4 (M = Ir (3a), Rh (3b) bis-NHC = methylenebis(N-2-methoxyethyl)imidazole-2-ylidene)) support a new mechanism, alternative to classical postulations, based on an outer-sphere model. Heterolytic splitting of the silane molecule by the metal centre and acetone (solvent) affords a metal hydride and the oxocarbenium ion ([R3Si–O(CH3)2]+), which reacts with the corresponding alkyne in solution to give the silylation product ([R3Si–CH=C–R]+), thus acetone acts as a silane shuttle transferring the silyl moiety from the silane to the alkyne. Finally, nucleophilic attack of the hydrido ligand over [R3Si–CH=C–R]+ affords selectively the β-(Z)-vinylsilane. The β-(Z)-selectivity has been explained on the grounds of the steric interaction between the silyl moiety and the ligand system resulting from the geometry of the approach that leads to β-(E)-vinylsilanes.

Keywords: Hydrosilylation • NHC • Carbene • Homogeneous Catalysis

Introduction

The synthesis of vinylsilanes has attracted considerable attention as a result of their increasing demand as key building blocks in synthetic organic chemistry.[1, 2] Vinylsilanes have been traditionally prepared by stoichiometric methods from organometallic reagents.[3] However, transition metal-catalysed hydrosilylation of terminal alkynes has become a highly sought-after route to vinylsilanes due to its efficiency and atom economy.[4]

Three possible isomers can be obtained from hydrosilylation of terminal alkynes (Figure 1). The most thermodynamically stable and usually major reaction product is the β-(E)-vinylsilane, while β-(Z)- and α-vinylsilanes are more elusive targets.[5] Catalyst design is, therefore, deemed crucial to overcome the thermodynamic stability of the β-(E)-vinylsilane and favour the less stable β-(Z)- and α-vinylsilanes.

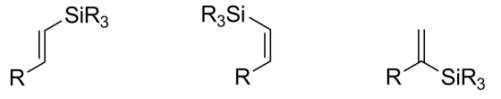

β-(E)-vinylsilane β-(Z)-vinylsilane α-vinylsilane

Figure 1. Possible products obtained from hydrosilylation of terminal alkynes.

A good understanding of the mechanisms involved in the selectivity of the process is essential to help the development of more selective catalysts. To our best knowledge, two main mechanisms have been proposed for the hydrosilylation of terminal alkynes. The first,

proposed by Chalk and Harrod (Chalk-Harrod mechanism),[6] entails the oxidative addition of the Si–H bond of the silane, followed by coordination of the alkyne and migratory insertion into the M–H bond. Subsequently, reductive elimination affords the β-(E)-vinylsilane. However, this mechanism does not explain dehydrogenative silylation products or the formation of β-(Z)-vinylsilanes usually observed when Ru, Rh, and Ir catalysts are employed. In order to justify the formation of these products, a new mechanism was proposed (modified Chalk-Harrod mechanism).[7] This postulates that the migratory insertion of the alkyne occurs into the M–Si bond instead of the M–H bond, thus rendering an M–alkenyl intermediate with the silyl moiety and the metal complex in relative cis positions (A) (Scheme 1). Then, a metal-assisted isomerisation from A to D is invoked in order to explain the formation of the β-(Z)-vinylsilane—the release of steric hindrance between the R3Si moiety and the metal complex being the driving force of the process. The isomerisation mechanisms proposed by Ojima and Crabtree independently have been ubiquitously employed as model to explain the formation of □-(Z)-vinylsilanes in the hydrosilylation of terminals alkynes.[8] The isomerisation process requires the formation of a metalacyclopropene (B) in the mechanism proposed by Crabtree et. al.,[9] or a zwitterionic carbene (C) in Ojima's mechanism,[10] as intermediates for the A-D isomerisation of the metal–alkenyl intermediate (Scheme 1). Therefore, isomerisation of A to the less sterically hindered intermediate D allows the formation the less thermodynamically stable β-(Z)-vinylsilane.

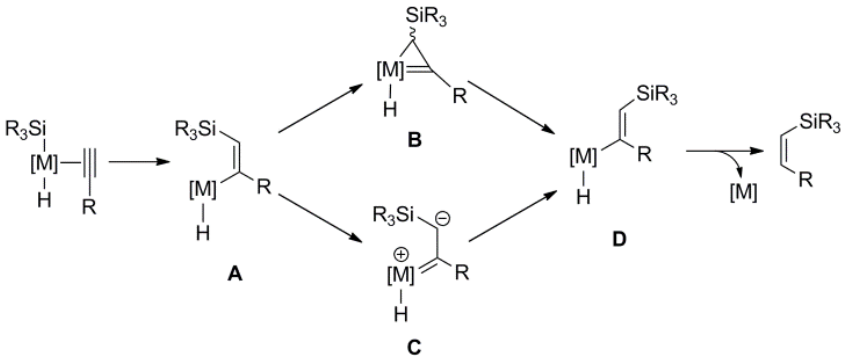

Scheme 1.Isomerization mechanism.

In a previous communication we described a hydrosilylation catalyst able to afford the □-(Z)-vinylsilane in excellent yields and selectivities.[11] The stereoselectivity of the process was tentatively explained as a consequence of the steric control exerted by the ligand system over the M-alkenyl intermediate, which isomerises according to a classical mechanism. However, trying to extend this reaction to other solvents we found out that acetone is the only solvent where the reaction takes place. This fact together with the increasing number of outer-sphere mechanisms recently published on iridium catalysed reactions[12] prompted us to study the role played by acetone in a catalytic cycle based on an outer-sphere mechanism.

In this work we disclose an outer-sphere mechanism for the hydrosilylation of terminal alkynes based on experimental data and theoretical calculations at the DFT level. Moreover, we have extended our previous communication[11] to an analogous rhodium catalyst. Its preparation

and full characterisation is described together with a comparative catalytic study of the iridium and rhodium catalysts.

Results and Discussion

Synthesis and characterization of complexes

Reaction of 1 with [MCl(COD)]2 (M = Rh, Ir; COD = 1,5-cyclooctadiene), sodium iodide and potassium acetate afforded [M(I)2(bis-NHC)(η2-CH3COO)] (M = Ir (2a), Rh (2b); bis-NHC = methylenebis(N-2-methoxyethyl)imidazole-2-ylidene)) as air stable orange solids. The reaction for the formation of complexes 2a and 2b entails a change in the oxidation state of the metal centres from M(I) to M(III) and concomitant loss of COD. The 1H NMR spectra of complex 2b in CDCl3 show a resonance corresponding to the methyl group of the η2-coordinated acetato ligand at δ 2.03 ppm (Scheme 2).

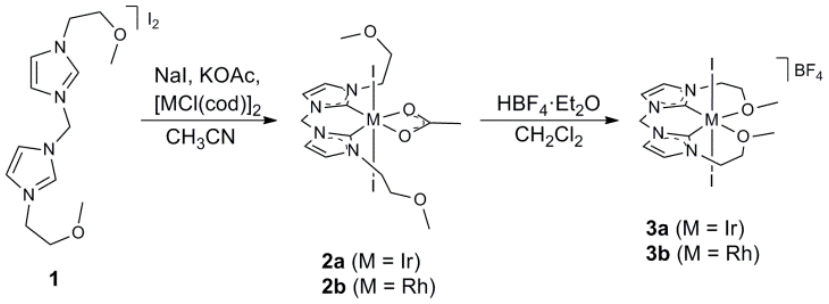

Scheme 2. Synthetic pathway to complexes 3a and 3b.

The protons corresponding to the imidazole rings appear as two doublets, with a coupling constant of 2 Hz, at δ 7.32 ppm and 7.05 ppm. The resonance assigned to the protons of the methylene bridge is observed as a singlet at δ 6.05 ppm. These NMR patterns are in agreement with the expected symmetry (C2v point group) in solution. In the 13C{1H} NMR spectra the most notable signal is that corresponding to the carbene carbon, which appears as a doublet centred at δ 154.3 ppm (JRh-C = 43 Hz). Moreover, the acetate ligand shows a doublet at δ 187.7 (JRh-C = 1.4 Hz) and a singlet at δ 24.8 ppm. These two resonances correspond, respectively, to the carboxylic and methyl carbons of the η2-coordinated acetato ligand. Complexes 2a and 2b were further characterized by X-ray crystallography as CH2Cl2 adducts. Figure 2 provides a view of 2a and 2b. Geometries of both Ir(III) and Rh(III) metal centres are octahedral, with iodido ligands at the apical positions, and two equatorial chelating acetato and bis-NHC-C,C ligands. The bridging methylene groups (C31) are situated slightly out of the equatorial plane of the metals (2a, 1.047(6) Å; 2b, 0.893(3) Å), while the η2-acetato ligands lie almost coplanar. Dihedral angle between the imidazole rings in 2a (33.8(2)º) is more pronounced in comparison to 2b (28.4(1)º). In addition, the side arms extend roughly symmetrically out of the equatorial planes.

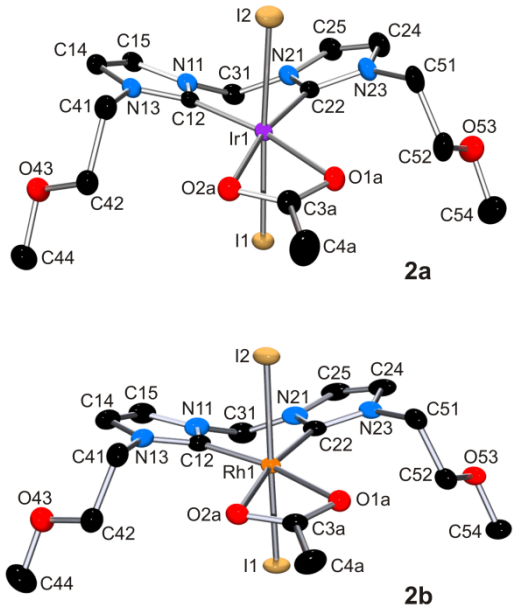

Figure 2. View of complexes [M(I)2(bis-NHC)(□□-CH3COO)] (M = Ir (2a), Rh (2b)) with atom-numbering schemes.

Complexes [M(I)2{κ-C,C,O,O-bis(NHC)}]BF4 (M = Ir (3a), Rh (3b)) were prepared in virtually quantitative yields by treatment of the corresponding 2a or 2b species with one equivalent of HBF4·Et2O in dry dichloromethane at 0 ºC (Scheme 2). Successful removal of the η2-acetato ligand was indicated by loss of the resonances corresponding to the acetate in 1H- and 13C-NMR spectra. Remarkably, in absence of the acetato ligand, coordination of the two oxygen atoms to the metal centre takes place as confirmed by X-ray diffraction studies of 3a and 3b (Figure 3). Coordination of the O-ethers at the sites occupied in 2a by the η2-acetato ligands modifies the equatorial coordination sphere of complexes 3a and 3b, with equatorial angles being closer to 90º and 180º. M–O bond distances (Ir1–O43 2.216(6) and Ir1–O53 2.208(6) Å) involving the coordinated sidearms are significantly longer for complexes 3a and 3b than those observed for the η2-acetato ligands in 2a and 2b. Tilt angle between both imidazole rings (24.8(5)º and 29.7(4)º) are in the range shown by 2a and 2b.

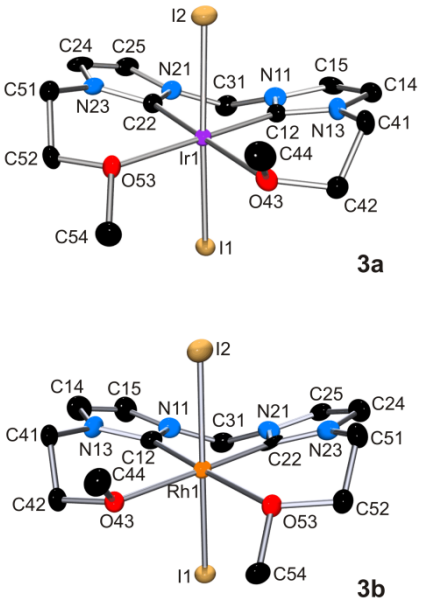

Figure 3. View of cations [M(I)2{κ-C,C,O,O-bis(NHC)}]+ (M = Ir (3a), Rh (3b)) with atom-numbering schemes. Both enantiomers are present in the unit cells.

1H NMR spectra of 3b show the resonance corresponding to the methylene bridge (C31 in Figure 3) as a singlet at δ 6.50 ppm, suggesting retention of the two-fold symmetry of these complexes in solution. The peaks corresponding to the –CH2O– and CH3O– groups undergo significant downfield shift in 1H NMR (in acetone-d6) from 2b to 3b, as a consequence of the coordination to the metal centre of the oxygen atoms in the wingtip groups. The resonance corresponding to the –CH2O– protons shifts δ 3.82–3.74 ppm in 2b to 4.42–4.37 ppm in 3b. The CH3O– resonance follows the same trend, thus shifting from 3.33 ppm in 2b to δ 4.06 ppm in 3b. 13C{1H} NMR spectra show a doublet for 2b at δ 146.8 ppm (JRh-C = 44 Hz) corresponding to the carbene carbons (C12 and C22. The presence of the BF4– anion was corroborated by 19F NMR, where a peak at δ –151.0 ppm was observed for 3b.

Catalytic study

At the outset of the catalytic study, we examined the reaction between phenylacetylene and triethylsilane with 3a as catalyst in order to optimise the reaction conditions. Remarkably, it was found that the reaction would only proceed in acetone. The use of other solvents such as toluene, dichloromethane, chloroform, methanol or acetonitrile afforded only traces of the hydrosilylated product. The reaction, initially attempted at room temperature, was found to be sluggish even in the presence of high catalyst loadings (c.a. 70% conversion after 5h with 10 mol% of 3a), whereas temperatures above 60 ºC bring about a loss of selectivity as the (Z)/(E) ratio decreases (from 22/1 at 50 ºC to 1.8/1 at 70 ºC) and more hydrogenated product is observed (from 8% at 50 ºC to 16% at 70 ºC). Complex 3a effectively catalyses the hydrosilyation of phenylacetylene with triethylsilane at 50 ºC with 5 mol% catalyst loading and 1.1 equivalents of the corresponding silane (Scheme 3). However, 3b was found to be considerably less active and selective than its iridium analogue (3a) under the reaction conditions and with the reagents previously mentioned (Table 1).

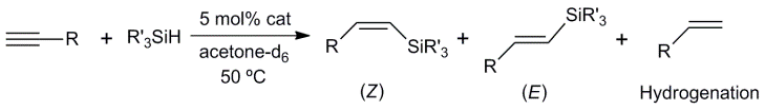

Scheme 3. Catalytic hydrosilylation of terminal alkynes.

Table 1. Hydrosilylation of Terminal Akynes with **3a**.

Alkyne (R)	Silane	(*Z*)	(*E*)	$RCH=CH_2$	Conversion (%)
Ph	Et_3SiH	86	7	7	100
	Me_2PhSiH	86	9	5	100
	$MePh_2SiH$	86	8	6	100
4-^{t}Bu-Ph	Et_3SiH	83	8	9	100
	Me_2PhSiH	94	2	4	100
	$MePh_2SiH$	84	8	8	100
4-MeO-Ph	Et_3SiH	93	5	2	100
	Me_2PhSiH	84	7	9	100
	$MePh_2SiH$	94	0	6	100
4-CF_3-Ph	Et_3SiH	93	5	2	100
	Me_2PhSiH	86	10	4	100
	$MePh_2SiH$	98	0	2	100
4-Me-Ph	Et_3SiH	92	7	1	100
	Me_2PhSiH	91	5	4	100
	$MePh_2SiH$	92	2	6	100
^{n}Heptyl	Et_3SiH	54	6	40	45
	Me_2PhSiH[b]	30	0	41	69
	$MePh_2SiH$	59	10	31	38
^{n}Butyl	Et_3SiH	74	13	13	100
	Me_2PhSiH	60	22	18	100
	$MePh_2SiH$	75	11	14	100

[a] Reaction conditions: 5h / 50 ºC / 5 mol% catalyst (**3a**) in acetone. [b] 29% of the vinylsilane is observed.

A detailed catalytic study was carried out under the above mentioned reaction conditions employing different silanes and a range of terminal alkynes, which were converted in excellent yields and selectivities to their corresponding β-(Z)-vinylsilanes using 3a as catalyst (Table 1). The best selectivities for 3a were obtained when the most sterically hindered silane (Ph2MeSiH) was employed; nonetheless, good results were also achieved with less encumbered silanes (PhMe2SiH and Et3SiH). Altogether, exceptional results were obtained with 3a for all the tested alkynes, but somewhat lower selectivities were found for aliphatic alkynes compared to their aromatic counterparts.

In the case of catalyst 3b, aliphatic alkynes were hydrosilylated in excellent yields and selectivities, especially employing Ph2MeSiH as silane. Remarkably, the use of Ph2MeSiH and PhMe2SiH with 3b as catalyst clearly improves the results obtained with 3a for 1-hexyne (nButyl; Table 2) and especially 1-nonyne (nHeptyl; Table 2). However, at variance with 3a, the use of Ph2MeSiH with 3b as catalyst leads to very low conversions with aromatic alkynes. In general, catalyst 3b shows an outstanding difference in activity upon modification of the silane substituents. As a matter of fact, good conversions and selectivities were obtained with PhMe2SiH, reaching total conversion after 5 h. Conversely, in the case of Ph2MeSiH and Et3SiH the conversions after 5 h were frequently below 50%. It is worth mentioning that those reactions which did not reach total conversion in 5 h are completed after extended reaction times, maintaining the initial selectivities (usually 36 h suffices). Therefore, total decomposition or deactivation of the catalyst can be discarded as cause of the low yields obtained using 3b as catalyst with HSiEt3 or HSiMePh2 after 5 h.

Table 2. Hydrosilylation of Terminal Akynes with **3b**.

Alkyne (R)	Silane	(*Z*)	(*E*)	$RCH=CH_2$	Conversion (%)
Ph	Et_3SiH	63	32	5	38
	Me_2PhSiH	76	24	0	100
	$MePh_2SiH$	74	26	0	39
4-^{t}Bu-Ph	Et_3SiH	88	11	<1	32
	Me_2PhSiH	89	11	0	100
	$MePh_2SiH$	85	15	0	39
4-MeO-Ph	Et_3SiH	91	7	1	53
	Me_2PhSiH	90	8	2	100
	$MePh_2SiH$	95	5	0	79
4-CF_3-Ph	Et_3SiH	57	42	1	70

	Me_2PhSiH	87	10	3	100
	$MePh_2SiH$	97	0	3	33
4-Me-Ph	Et_3SiH	80	17	3	45
	Me_2PhSiH	90	10	0	100
	$MePh_2SiH$	100	0	0	44
^{n}Heptyl	Et_3SiH	94	3	3	88
	Me_2PhSiH	88	10	2	100
	$MePh_2SiH$	94	4	2	100
^{n}Butyl	Et_3SiH	95	5	0	88
	Me_2PhSiH	79	11	10	100
	$MePh_2SiH$	92	6	2	100

[a] Reaction conditions: 5h / 50 ºC / 5 mol% catalyst (**3b**) in acetone.

Kinetic experiments performed with representative alkynes (R = 4-CF3-Ph, 4-MeO-Ph and nHeptyl) are shown in Figure 4. Remarkably, a significant drop in activity, mainly in the case of catalyst 3b, is observed when the more sterically hindered Ph2MeSiH is employed instead of PhMe2SiH. This effect is especially remarkable for R = 4-CF3-Ph (Figure 4), as the conversion falls from 80% to 11% after 90 min. However, as a general rule the best selectivities are obtained with Ph2MeSiH and decrease with the less sterically hindered PhMe2SiH, this effect being more noticeable in the case of 3b (Table 1 and Table 2).

The reaction rates obtained for aromatic alkynes using 3a as catalyst with Ph2MeSiH and PhMe2SiH are higher than those for 3b with the same alkynes, except in the case of the 4-methoxy derivative, where 3b with PhMe2SiH shows a greater reaction rate than that of 3a with Ph2MeSiH (89% and 79% at 90 min, respectively). In the case of aliphatic alkynes, namely 1-nonyne, the reaction with PhMe2SiH is finished within the first 30 minutes with 3b as catalyst. Conversely, the same reaction after 5h with catalyst 3a does not reach total conversion (Table 1). Therefore, it can be concluded that iridium catalyst 3a is significantly more active than 3b for the hydrosilylation of aromatic alkynes, whereas the trend observed for aliphatic alkynes is the opposite; 3b is remarkably more active than its iridium analogue 3a.

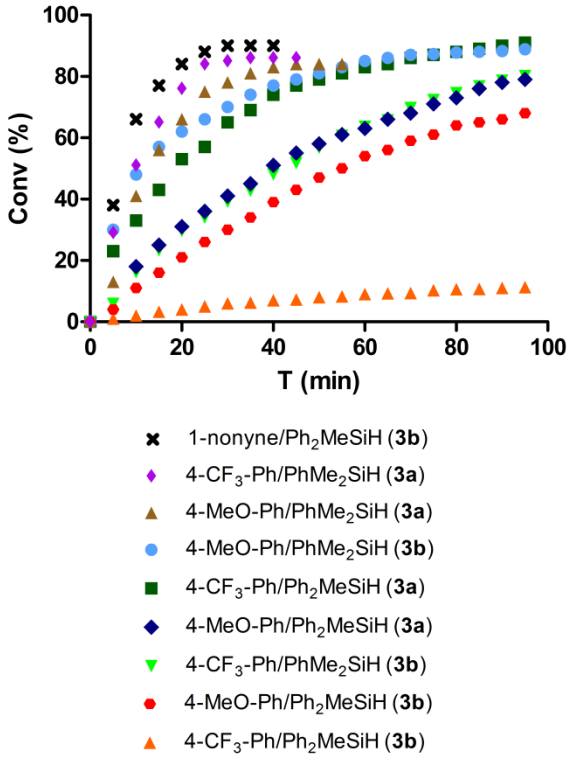

Figure 4. Kinetic experiments performed with representative alkynes (reaction conditions: 50 ºC, 5 mol% catalyst).

Mechanistic proposal

In the search for a deeper understanding of the catalytic cycle that could explain the key role of acetone, the investigation was extended to theoretical calculations at the DFT level. Initial calculations aimed at achieving computational support for a classic mechanism, based on a cycle consistent with the modified Chalk-Harrod mechanism. Therefore, oxidative addition of the silane followed by coordination of the alkyne and insertion into the M–Si bond is required. However, theoretical calculations show that M(V) (M = Ir or Rh) species resulting from oxidative addition of R3Si–H to 3a or 3b are not stable due to the high trans effect of the hydrido ligand trans to one of the NHCs (Scheme 4-a). A second possibility that entails prior coordination of the alkyne to give a vinylidene (Scheme 4-b) can be excluded as no reaction was observed between alkynes and complexes 3a or 3b in absence of silane under catalytic conditions—not even at temperatures as high as 80 ºC. Consequently, once all possibilities of classical mechanisms have been ruled out, a solvent assisted outer-sphere mechanism seems to be the most likely alternative.

What could the connection between acetone and hydrosilylation be? As an answer to this question, we have proposed a new mechanism for hydrosilylation of terminal alkynes based on a acetone assisted heterolytic splitting of silane (Scheme 4-c), where the reaction solvent (acetone) transfers the R3Si+ moiety from the silane to the terminal alkyne by means of an oxocarbenium ion. In this line, recent reports by Brookhart et. al. on hydrosilylation of ketones show evidences of the formation of an oxocarbenium ion, generated by reaction of a ketone with R3Si+ (resultant of the abstraction of a hydride from R3SiH by the metal centre).[13]

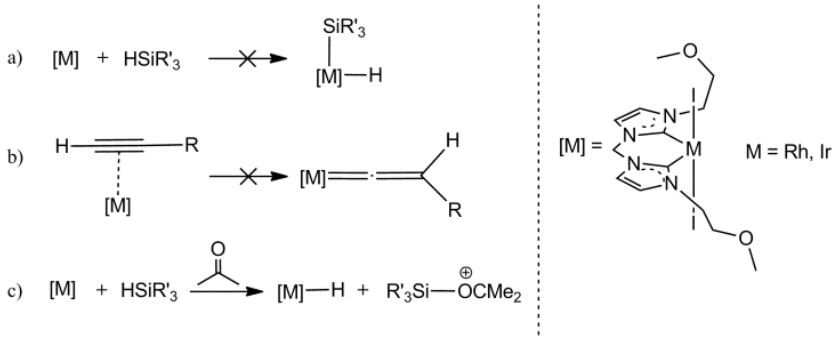

Scheme 4. Possible initial steps of the catalytic cycle.

The calculations were carried out at the B3LYP level using the def2-SVP basis set for all atoms and the associated core pseudopotentials for the metals and iodine. Due to the decisive role of acetone, up to two molecules were considered in the calculations of the reaction mechanism. Single point calculations using a continuum model on the gas-phase optimised structures were carried out in order to simulate solvent effects with a dielectric constant for acetone of 20.493. In this computational study, all reported energies are relative to the reactants (3a and the corresponding isolated molecules) and include the solvent correction.

This mechanism starts with the dissociation of the two ether functions in the wingtip groups, followed by coordination to the metal centre of an acetone molecule and the silane in an end-on fashion, yielding intermediate C-2, which is 9.5 kcalmol-1 less stable than the reactants (see Figure 5). It is worth mentioning that the crystal structure of a complex with a triethylsilane coordinated end-on through the hydrogen atom to an iridium centre, comparable to intermediate C-2, has been recently reported. The authors, based on DFT studies, suggest a greater electrophilicity at the Si atom in a η1-H(Si) species compared to its analogue η2-H(Si).[14] Remarkably, our theoretic calculations show that acetone coordinates to the metal better than the ether at the wingtip groups in solution; consequently, all the calculated metal complexes bear an acetone molecule. This may force the η1-H(Si) coordination of the silane, resulting in an increase of electrophilicity at the silicon atom. Subsequently, the oxygen lone pair of another acetone molecule can interact with the back side of the silane molecule forming species C-3. The formation of the oxocarbenium ion and the hydride takes place via the C-4-TS (Figure 6), affording an activation barrier of 12.1 kcalmol-1. This transition structure can be described as a SN2 silyl transfer to the oxygen and concomitant formation of the Ir–H bond. Although the formation of C-5 is an endothermic process (+5.0 kcalmol-1), it can be achieved at ambient temperature.

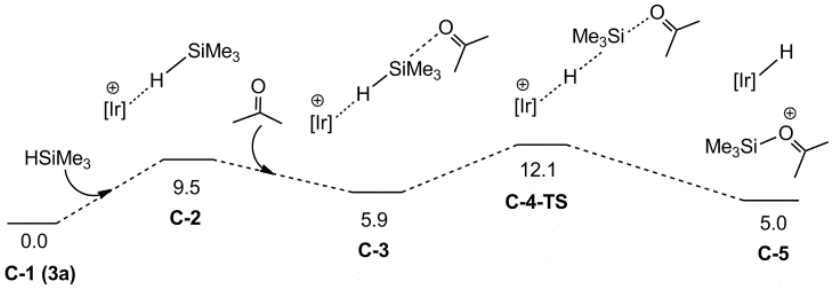

Figure 5. DFT calculated relative energy (ΔE in kcalmol-1) profile for the heterolytic splitting of SiMe3.

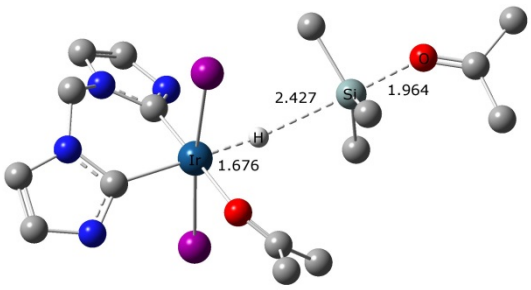

Figure 6. DFT optimized structure of C-4-TS, leading to the iridium hydrido complex and oxocarbenium ion. Wingtip groups and hydrogen atoms have been omitted for clarity.

After formation of the M–H bond and the oxocarbenium ion, three possible reaction pathways have been considered (Scheme 5).

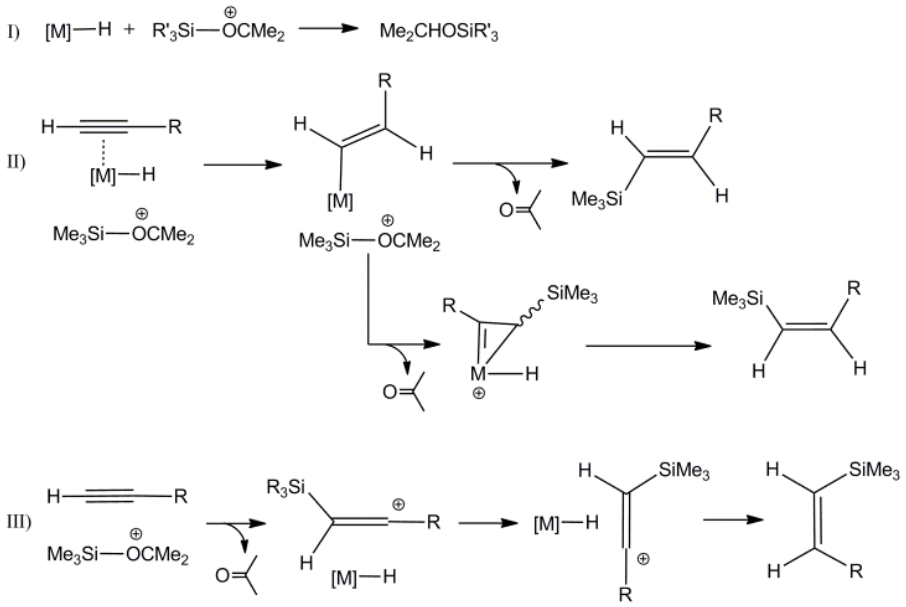

Scheme 5. Possible non-classical reaction pathways.

First, acetone hydrosilylation is obtained by nucleophilic attack of the hydride over the oxocarbenium ion. In Figure 7 the calculated energy profile is shown, revealing a very low activation barrier (8.3 kcalmol-1) for the hydride transfer from the metal to the carbon (I-2-TS). Although this process is exothermic (–9.2 kcalmol-1), the energy barrier for the reverse reaction is of only 17.5 kcalmol-1. Therefore, in the absence of alkyne or other reactants, hydrosilylation of acetone is a kinetically and thermodynamically favoured reaction. As a matter of fact, this process is experimentally observed in the absence of alkyne. However, as a

reversible process, the existence of a competitive pathway (reaction of the oxocarbenium ion with alkynes) may yield a different product.

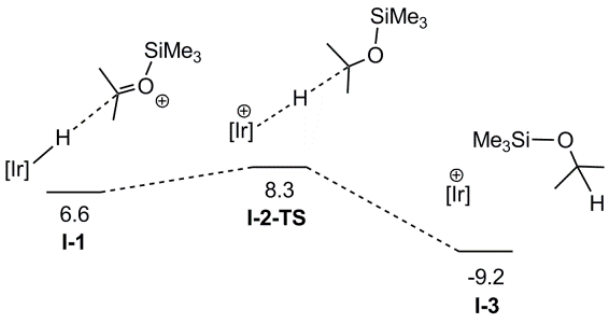

Figure 7. DFT calculated relative energy (ΔE in kcalmol-1) profile for acetone hydrosylilation.

Two possible reaction mechanisms have been considered for the reaction of the hydrido complex and oxocarbenium ion with an alkyne. In mechanism II (Scheme 5), coordination of the alkyne to the metal followed by insertion into the M–H bond is proposed; however, this mechanism may yield only the β-(E)- or α- but not the β-(Z)-vinylsilane. Alternatives through a metallacycle intermediate and further cis-trans isomerisation have been proposed[9] but the calculated relative energy for the metallacycle is too high (22.8 kcalmol-1) and therefore, this way can be discarded.

Another alternative mechanism is the reaction of the oxocarbenium ion with the alkyne to yield a β-silyl carbocation (Scheme 5-III). The existence of such species has been previously reported. The stability of this carbocation can be attributed to the large hyperconjugative nature of the β-silyl effect.[15] Therefore, acetone acts as a silane shuttle transferring the R3Si+ moiety from the silane to a molecule of alkyne by means of an oxocarbenium ion. The energy profile for the silyl transfer from the oxocarbenium ion to the alkyne to form III-3 is shown in Figure 8, and features an activation barrier of 15.7 kcalmol-1.

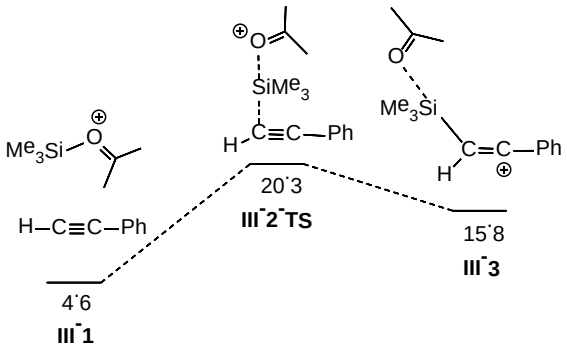

Figure 8. DFT calculated relative energy (ΔE in kcalmol-1) profile for the silyl transfer from the oxocarbenium ion to the alkyne.

The carbocation resulting from the silylation of the alkyne reacts with the hydrido complex without previous coordination due to steric interaction between them. Therefore, the vinylsilane is formed by nucleophilic attack of the hydride over the carbocation. Two geometries are conceivable for the approach of the carbocation. The first possibility features the Me3Si moiety pointing outside the metal complex (III-5-TS, Figure 10), which leads to the

formation of the β-(Z)-vinylsilane with an activation barrier of 19.1 kcalmol-1. However, in the second approach, the Me3Si (trans positioned with respect to the phenyl group) points toward the metal centre (III-5-TS', see Figure 10), the activation barrier being 30.9 kcalmol-1 and leading to the β-(E)-vinylsilane. Both processes are very exothermic, the β-(E)-vinylsilane being the thermodynamically favoured product (Figure 9).

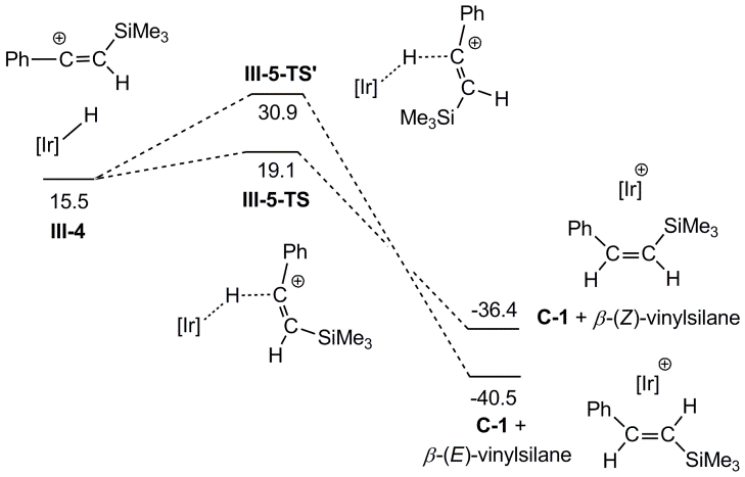

Figure 9. DFT calculated relative energy (ΔE in kcalmol-1) profile for the nucleophilic attack of the hydride to the carbonation to yield β-(Z)- and β-(E)- vinylsilanes.

The origin of the β-(Z)-selectivity can be explained on the grounds of the greater steric congestion in III-5-TS' compared to III-5-TS, consequence of the silyl moiety interacting with the two iodido ligands in the apical positions and the wingtip groups in the equatorial plane as it is supported by the different energy barrier between both process.

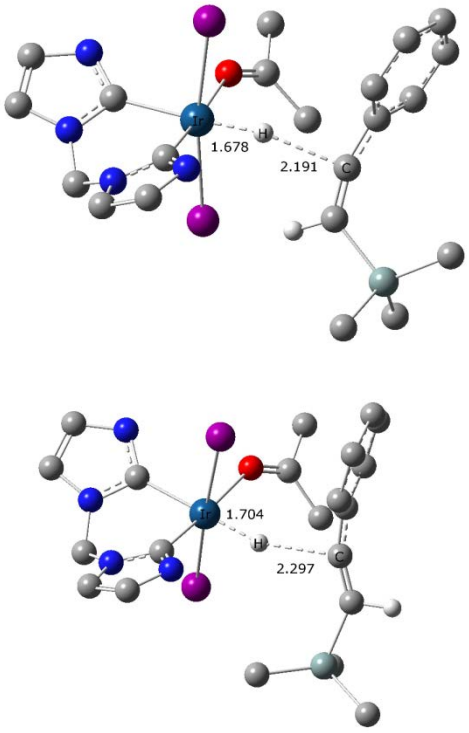

Figure 10. DFT optimized structure of III-5-TS (up) and III-5-TS' (down) leading to the β-(Z)-vinylsilane and β-(E)-vinylsilane, respectively. Wingtip groups and hydrogen atoms have been omitted for clarity.

Conclusions

We have developed a straightforward method for the synthesis of cationic bis(NHC)-C,C,O,O iridium(III) and rhodium(III) complexes (3a and 3b). These complexes showed good activities in the hydrosilylation of terminal alkynes and excellent selectivities towards β-(Z)-vinylsilanes only when acetone was used as solvent. Remarkably, iridium complex 3a performs better in the hydrosilylation of aromatic alkynes than rhodium complex 3b. Conversely, 3b shows better selectivities and activities than 3a in the hydrosilylation of aliphatic alkynes.

The reaction mechanism was investigated in a combined computational and experimental study. The possibility of a classical mechanism was discarded as (i) the oxidative addition of the Si–H bond to the rhodium or iridium centre was found to be unfeasible by calculations at the DFT level and (ii) it was found experimentally that alkynes do not react with 3a or 3b.

An outer-sphere mechanism for the hydrosilylation of terminal alkynes was proposed based on Si–O interactions between the silane and the solvent (acetone). The mechanism proposal is based on three main steps, (i) the heterolytic splitting of the silane molecule by the metal centre and the acetone molecule, (ii) the reaction of the resulting oxocarbenium ion ([R3Si–O(CH3)2]+) with the corresponding alkyne to give the silylation product ([R3Si–CH=C–R]+), and (iii) nucleophilic attack of the hydrido ligand over [R3Si–CH=C–R]+. The β-(Z)-selectivity of the reaction is explained as a consequence of the higher steric interaction resulting from the geometry of the approach that leads to β-(E)-vinylsilanes.

This mechanism proposal represents the first example of an outer-sphere mechanism for the hydrosilylation of terminal alkynes. The development of new catalytic systems operating through outer-sphere mechanisms based on Si–O interactions, which could direct the selectivity of the hydrosilylation of alkynes towards the desired vinylsilane, are currently being investigated in our group.

Experimental Section

General Information: All manipulations were performed using standard Schlenk techniques under an argon atmosphere, except where otherwise noted. All complexes after their formation were treated under aerobic conditions. Solvents were obtained dried from a solvent purification system from Innovative Technology Inc. Salt 1 and complexes 2a and 3a have been prepared according to a synthetic procedure recently reported by us.[11] All other reagents were used as received. NMR spectra were recorded on Bruker Avance 300 MHz, Bruker ARX 300 or Bruker Avance 400 MHz spectrometers. The chemical shifts are given as dimensionless δ values and are frequency referenced relative to residual solvent peaks for 1H and 13C. Coupling constants J are given in Hertz as positive values regardless of their real individual signs. The multiplicity of the signals is indicated as "s", "d", or "m" for singlet, doublet, or multiplet, respectively. Mass spectra and high-resolution mass spectra were obtained on a esquire 3000+ with ion trap detector interfaced on an Agilent 1100 HPLC analyzer, in

electrospray (ES) mode unless otherwise reported. Elemental analyses C/H/N were carried out in a Perkin-Elmer 2400 CHNS/O analyzer.

Synthesis of methylenebis(N-2-methoxyethyl)imidazole-2-ylidene)acetato(diiodo)Rhodium(III) (2b). A mixture of [Rh(μ-Cl)(COD)]2 (0.123 g, 0.25 mmol), 1 (0.260 g, 0.5 mmol), NaI (0.70 g, 5.0 mmol), KOAc (0.65 g, 6.5 mmol) and CH3CN (15 mL) was refluxed for 3 days, after which time the solvent was evaporated under reduced pressure. The remaining residue was dissolved in CH2Cl2, and any insoluble impurities were filtered off. The solution was concentrated to ca. 1 mL and the product precipitated with diethyl ether. The solid was washed with diethyl ether (3 × 10 mL) and dried in vacuo to give 0.15 g (88%) of an orange solid. 1H NMR (Acetone, 400 MHz): δ 7.48 (d, JH-H = 2.1 Hz, 2H, CHim), 7.42 (d, JH-H = 2.1 Hz, 2H, CHim), 6.27 (s, 2H, NCH2N), 4.71–4.58 (m, 4H, CH2N), 3.82–3.74 (m, 4H, CH2O), 3.33 (s, 6H, CH3O), 1.82 (s, 3H, CH3AcO).1H NMR (CDCl3, 400MHz): δ 7.32 (d, 2H, JH-H = 2Hz, CHim), 7.05 (d, 2H, JH-H = 2Hz, CHim), 6.05 (s, 2H, NCH2N), 4.71–4.65 (m, 4H, NCH2), 3.85–3.81 (m , 4H, CH2O), 3.36 (s, 6H, CH3O), 2.03 (s, 3H, CH3AcO). 13C{1H} NMR plus APT (CDCl3, 101 MHz): δ 187.7 (d, JRh-C = 1.4 Hz, CCOO–), 154.3 (d, JRh-C = 43 Hz, NCimN), 125.4 (CHim), 119.6 (CHim), 72.4 (OCH2), 63.3 (NCH2N), 58.9 (CH3O), 51.1 (CH2N), 24.8 (CH3COO–). Anal. Calcd. for C15H24I2RhN4O4 (680.89): C, 26.45; H, 3.55; N, 8.23. Found: C, 26.76; H, 3.56; N, 8.49.

Synthesis of methylenebis(N-2-methoxyethyl-κO,κO')imidazole-2-ylidene)(diiodo)Rhodium(III) tetrafluoroborate (3b). To a solution of 2b (0.35 g, 0.51 mmol) in dry CH2Cl2 (30 mL) at 0 ºC, HBF4 (75 μL, 0.55 mmol) was added dropwise under Argon, the mixture was stirred for 1 h and allowed to warm to room temperature, thus affording an orange suspension. Subsequently, the solvent was evaporated under reduced pressure until a volume of ca. 1mL and precipitated with Et2O (10 mL). The resulting residue was washed with diethyl ether (3 × 10 mL) to afford 0.30 g (83%) of an orange solid. 1H NMR (Acetone-d6, 400MHz): δ 7.72 (d, 2H, JH-H = 2Hz, CHim), 7.70 (d, 2H, JH-H = 2Hz, CHim), 6.50 (s, 2H, NCH2N), 4.80–4.74 (m, 4H, CH2N), 4.42–4.37 (m, 4H, OCH2), 4.06 (s, 6H, CH3O). 13C{1H} NMR (Acetone-d6, 101 MHz): δ 146.8 (d, JRh-C = 44 Hz, NCimN), 124.6 (CHim), 122.1 (CHim), 76.7 (OCH2), 67.6 (CH3O), 62.5 (NCH2N), 49.6 (CH2N). 19F NMR (Acetone-d6, 282 MHz): δ –151.0. Anal. Calcd. for C13H20BF4I2RhN4O2 (707.88): C, 22.06; H, 2.85; N, 7.92. Found: C, 22.10; H, 2.77; N, 8.16.

NMR studies of the hydrosilylation of alkynes. 6.0 mg (7.5 × 10–3 mmol) of the corresponding catalyst precursor, 3a or 3b, were dissolved in 0.5 mL of acetone-d6 in a NMR tube. Subsequently, 0.16 mmol of the silane, 0.15 mmol of the corresponding alkyne and mesitylene (21.0 μL, 0.15 mmol) as internal standard were added. The NMR tube was then closed under Argon and placed in and oil bath for 5h at 50 ºC. Yields and selectivities were calculated by 1H NMR. The different isomers were unambiguously identifies by means of the 3JH-H coupling constants of the vinylic protons.

X-ray Crystallography. Intensity data of 2a, 2b, 3a and 3b were collected on a Bruker Kappa APEX2 diffractometer (Mo Kα 0.71069 Å, graphite-monochromator). Data reduction and cell refinements were carried out using the APEX2 software package.[16] All the structures were solved by direct methods and refined by full-matrix least-squares based on F2 using the SHELXL-97 and WinGX programs.[17] Positions of all non-hydrogen atoms were deduced from difference Fourier maps and refined anisotropically. Distance and/or thermal restraints were

applied to CH2Cl2 (2a), BF4 (3a) and N13, N22, O53, F12, f14 (3b). Hydrogen atoms were positioned in geometrically calculated positions and refined with isotropic displacement parameters according to the riding model.

Crystal data for [Ir(I)2(bis-NHC)(η2-CH3COO)]·CH2Cl2 (2a): [C16H25Cl2I2IrN4O4], orthorhombic, Pbca, a = 16.0598(12) Å, b = 13.9481(10) Å, c = 22.4432(17) Å, Z = 8, Mr = 854.3 g mol–1, V = 5027.4(6) Å3, Dcalcd = 2.257 g cm–3, λ(Mo Kα) = 0.71073 Å, T = 100 K, μ = 8.008 mm–1, 53124 reflections collected, 6809 observed (Rint = 0.0435), R1(Fo) = 0.0273 [I > 2σ(I)], wR2 (Fo2) = 0.0700 (all data), GOF = 1.037. CCDC 953145.

Crystal data for [Rh(I)2(bis-NHC)(η2-CH3COO)]·CH2Cl2 (2b): [C16H25Cl2I2N4O4Rh], triclinic, P–1, a = 8.6375(7) Å, b = 12.0197(10) Å, c = 13.3547(11) Å, α = 97.0160(10)º, β = 108.7340(10)º, γ = 105.6760(10)º, Z = 2, Mr = 765.01 g mol–1, V = 1230.56(18) Å3, Dcalcd = 2.065 g cm–3, λ(Mo Kα) = 0.71073 Å, T = 100 K, μ = 3.448 mm–1, 13529 reflections collected, 6234 observed (Rint = 0.0207), R1(Fo) = 0.0217 [I > 2σ(I)], wR2 (Fo2) = 0.0561 (all data), GOF = 1.038. CCDC 953146.

Crystal data for [Ir(I)2{η4:κ-O,κ-O-bis(NHC)}](BF4) (3a): [C13H20BF4I2IrN4O2], triclinic, P–1, a = 8.1369(6) Å, b = 12.3989(10) Å, c = 13.1088(10) Å, α = 62.7780(10)º, β = 76.3250(10)º, γ = 75.5850(10)º, Z = 2, Mr = 797.14 g mol–1, V = 1127.43(15) Å3, Dcalcd = 2.348 g cm–3, λ(Mo Kα) = 0.71073 Å, T = 100 K, μ = 8.706 mm–1, 12465 reflections collected, 5718 observed (Rint = 0.0220), R1(Fo) = 0.0482 [I > 2σ(I)], wR2 (Fo2) = 0.1276 (all data), GOF = 1.031. CCDC 953147.

Crystal data for [Rh(I)2{η4:κ-O,κ-O-bis(NHC)}](BF4) (3b): [C13H20BF4I2N4O2Rh], triclinic, P–1, a = 8.6767(13) Å, b = 10.3696(15) Å, c = 12.4048(18) Å, α = 84.859(2)º, β = 70.430(2)º, γ = 77.625(2)º, Z = 2, Mr = 707.85 g mol–1, V = 1027.0(3) Å3, Dcalcd = 2.289 g cm–3, λ(Mo Kα) = 0.71073 Å, T = 100 K, μ = 3.889 mm–1, 11996 reflections collected, 4702 observed (Rint = 0.0255), R1(Fo) = 0.0597 [I > 2σ(I)], wR2 (Fo2) = 0.1434 (all data), GOF = 1.084. CCDC 953146.

These data can be obtained free of charge from the Cambridge Crystallographic Data Centre via www.ccdc.cam.ac.uk/data_request/cif.

Acknowledgements

This work was supported by the Spanish Ministry of Economy and Competitiveness (MINECO/FEDER) (CONSOLIDER INGENIO-2010, CTQ2011-27593 projects, and “Ramón y Cajal” (P.J.S.M.) and “Juan de la Cierva” (M.I.) programs) and the DGA/FSE (E07). One of the authors (V. P.) thankfully acknowledges the resources from the supercomputer "Terminus", technical expertise and assistance provided by the Institute for Biocomputation and Physics of Complex Systems (BIFI) - Universidad de Zaragoza.

[1] (a) I. Ojima, in The Chemistry of Organic Silicon Compounds (Eds: S. Patai, Z. Rappoport), Wiley, New York, 1989, p 1479; (b) Ojima, I.; Li, Z.; Zhu, J. in The Chemistry of Organic Silicon Compounds (Eds: Z. Rappoport, Y. Apeloig), Wiley, New York, 1998, p 1687.

[2] G. W. Gribble, J. J. Li, in Palladium in Heterocyclic Chemistry: a Guide for the Synthetic Chemist (Eds: G. W. Gribble, J. J. Li), Elsevier Science Ltd., Oxford, 2006, p 12.

[3] For examples see: (a) J. D. Sunderhaus, H. Lam, G. B. Dudley, Org. Lett. 2003, 8, 4571–4573; (b) K. Murakami, H. Yorimitsu, K. Oshima, J. Org. Chem. 2009, 74, 1415–1417.

[4] (a) For a reviews see: B. Marciniec, C. Pietraszuk, I. Kownacki, M. Zaidlewicz, in Comprehensive Organic Functional Group Transformations (Eds: A. R. Katrizky, J. K. Taylor) Elsevier, Oxford, 2005, p. 941; (b) P. Pawluć, W. Prukala, B. Marciniec, Eur. J. Org. Chem. 2010, 219–229; (c) D. Lin, E. Anderson, Synthesis 2012, 44, 983–1010.

[5] (a) A. K. Roy, Adv. Organomet. Chem. 2008, 55, 1–59; (b) B. Marciniec, K. H. Maciejewski, C. Pietraszuk, P. Pawluć, Hydrosilylation: A Comprehensive Review on Recent Advances (Ed: B. Marciniec) Springer, London, 2008.

[6] A. J. Chalk, J. F. Harrod, J. Am. Chem. Soc. 1965, 87, 16–21.

[7] (a) J. F. Harrod, A. J. Chalk, in Organic Synthesis via Metal Carbonyls (Eds: I. Wender, P. Pino), John Wiley & Sons Ltd., New York, 1977; Vol. 2, p 673; (b) T. D. Tilley, in The Chemistry of Organic Silicon Compounds (Eds: S. Patai, Z. Rappoport), John Wiley & Sons Ltd.: New York, 1989, p 1415; (c) I. Ojima, in The Chemistry of Organic Silicon Compounds (Ed. S. Patai, Z. Rappoport), John Wiley & Sons Ltd.: New York, 1989, p 1479; (d) M. A. Schroeder, M. S. Wrighton, J. Organomet. Chem. 1977, 128, 345–358; (e) C. L. Reichel, M. S. Wrighton, Inorg. Chem. 1980, 19, 3858–3860; (f) C. L. Randolph, M. S. Wrighton, J. Am. Chem. Soc. 1986, 108, 3366–3374; (g) A. Milan, E. Towns, P. M. J. Maitlis, Chem. Soc. Chem. Commun. 1981, 673–674; (h) A. Milan, M.-J. Fernandez, P. Bentz, P. M. Maitlis, J. Mol. Catal. 1984, 26, 89–104; (i) I. Ojima, M. Yatabe, T. Fuchikami, J. Organomet. Chem. 1984, 260, 335–346.

[8] For examples see: (a) J. W. Faller, D. G. D'Alliessi, Organometallics 2002, 21, 1743–1746; (b) R. H. Crabtree, New J. Chem. 2003, 27, 771–772; (c) M. V. Jiménez, J. J. Pérez-Torrente, M. I. Bartolomé, V. Gierz, F. J. Lahoz, L. A. Oro, Organometallics 2008, 27, 224–234.

[9] R. S. Tanke, R. H. Crabtree, J. Am. Chem. Soc. 1990, 112, 7984–7989.

[10] I. Ojima, N. Clos, R. J. Donovan, P. Ingallina, Organometallics 1990, 9, 3127–3133.

[11] M. Iglesias, M. Pérez-Nicolás, P. J. Sanz Miguel, V. Polo, F. J. Fernández-Alvarez, J. J. Pérez-Torrente, L. A. Oro, Chem. Commun. 2012, 48, 9480–9482.

[12] (a) M. Martín, E. Sola, S. Tejero, J . A. López, L. A. Oro, Chem. Eur. J. 2006, 12, 4057–4068; (b) M. Martín, E. Sola, S. Tejero, J. L. Andrés, L. A. Oro, Chem. Eur. J. 2006, 12, 4043–4056; (c) G. E. Dobereiner, A. Nova, N. D. Schley, N. Hazari, S. J. Miller, O. Eisenstein, R. H. Crabtree, J. Am. Chem. Soc. 2011, 133, 7547–7562; (d) I. Mena, M. A. Casado, V. Polo, P. García-Orduña, F. J. Lahoz, L. A. Oro, Angew. Chem. Int. Ed. 2012, 51, 8259–8263; (e) R. Lalrempuia, M. Iglesias, V. Polo, P. J. Sanz Miguel, F. J. Fernández-Alvarez, J. J. Pérez-Torrente, L. A. Oro, Angew. Chem. Int. Ed. 2012, 51, 12824–12827; (f) P. C. Roosen, V. A. Kallepalli, B. Chattopadhyay, D. A. Singleton, R. E. Malezca Jr, M. R. Smith III, J. Am. Chem. Soc. 2012, 134, 11350–11353; (g) W. W. N. O, A. J. Lough, R. H. Morris, Organometallics 2012, 31, 2152–2165; (h) N. D. Schley, S. Halbert, C. Raynaud, O. Eisenstein, R. H. Crabtree, Inorg. Chem. 2012, 51, 12313–12323.

[13] S. Park, M. Brookhart, Organometallics 2010, 29, 6057–6064.

[14] J. Yang, P. S. White, C. K. Schauer, M. Brookhart, Angew. Chem. Int. Ed. 2008, 47, 4141–4143.

[15] V. Gabelica, A. J. Kresge J. Am. Chem. Soc. 1996, 118, 3838-3841.

[16] APEX2 Bruker AXS Inc., Madison, Wisconsin, USA, 2011.

[17] (a) G. M. Sheldrick, SHELXS-97 and SHELXL-97; University of Göttingen, Germany, 1997; (b) L. J. Farrugia, WinGX; University of Glasgow, Great Britain, 1998.